Materials Science-Poland, 42(2), 2024, pp. 160-177
http://www.materialsscience.pwr.wroc.pl/
DOI: 10.2478/msp-2024-0026

Shear and flexural strength of reinforced concrete beams made with recycled coarse aggregate concrete

Hassan M. Magbool[1,*], Mohamed Gamil[2], Mohamed S. Issa[2], Ahmed A. El-Abbasy[1]

[1]Civil and Architectural Engineering Department, College of Engineering and Computer Science, Jazan University, Jazan, Saudi Arabia

[2]Housing and Building National Research Center, Reinforced Concrete Research Department, Giza, Egypt

Concrete production relies heavily on minerals and nonrenewable resources, specifically natural aggregate. However, waste from construction and demolition projects accumulates in landfills, contaminating the air and groundwater. This affects economies by increasing annual expenditures. The solution can be found by employing concrete made from recycled concrete aggregates (RCA). In this study, finite element (FE) simulations with ABAQUS software are conducted to investigate the shear and flexural behavior of beams made of RCA. The accuracy and dependability of the FE models are validated by contrasting the FE results with those of previous experimental tests. Sixty FE models with different parameters, including various coarse natural aggregate replacement levels (i.e., 0%, 25%, 50%, 75%, and 100%), compressive strengths (i.e., 25, 35, and 40 MPa), and reinforcement rebar diameters (i.e., 14, 16, and 18 mm), are numerically investigated. Moreover, additional experimental results reported in the literature (30 for shear and 61 for flexural tests) are utilized to verify the American Concrete Institute Code (ACI318-19), the Saudi Building Code (SBC304-18), and the Egyptian Code of Practice (ECP203-2020) provisions for shear and flexure capacity. Shear results showed that the load capacity decreased with increased RCA replacements. However, the effect of RCA on the flexural capacity is limited. The project proves that the provisions of the ACI318-19, SBC304-18, and ECP203-2020 codes for calculating the shear and flexural capacities can still be used for beams made of RCA.

Keywords: *flexural capacity, RC beams, recycled concrete aggregate, shear capacity*

1. Introduction

Minerals and nonrenewable resources are extensively used to produce concrete, especially natural aggregate. Concrete is a highly crucial element in building demolition operations. However, the waste generated from construction and demolition projects rapidly accumulates in landfills. This phenomenon adversely affects the ecosystem by causing air and groundwater contamination. The annual expenditures of millions of dollars to transport concrete waste from large towns to designated landfill sites, remove concrete debris from construction and demolition locations, and perform the appropriate burial procedures will further strain the economies of countries [1, 2]. Every year, the European Union produces more than 450 million tons of demolition waste, or approximately 1 ton per person [3]. However, the amount of demolition waste is increasing at unacceptable rates due to the ongoing conflicts in many regions of the world. These nations lack proper monitoring of demolition waste and face financial constraints that hinder appropriate disposal efforts, which has significant adverse effects on the environment, people's health, and safety [4, 5].

Envision a world where we can construct structures that can withstand the loads applied over time while also preserving our planet. This vision is closer than you might imagine, and the solution lies in utilizing concrete made from recycled concrete aggregates (RCA) [6, 7]. Our research is focused on achieving a more sustainable and eco-friendly future. From the perspective of environmental sustainability, it is crucial to use waste concrete as RCA because the aggregate typically makes up 60%–80% of the concrete volume [8, 9]. Recycled aggregate refers to aggregates that have been recycled from previous building projects. Some reprocessing processes include crushing or grading aggregate to meet the required standards.

* E-mail: h.magbool@jazanu.edu.sa

An appropriate solution to achieve the objective of protecting non-renewable resources is to employ recycled aggregate in civil engineering applications [10, 11].

Researchers undertook numerous investigations to examine the effect of using RCA in concrete. Abedalqader et al. [12] experimentally examined the effect of adding recycled asphalt pavement (RAP) and RCA on the concrete mechanical characteristics after being exposed to a range of temperatures (20 °C, 200 °C, 400 °C, and 500 °C) and investigated the compressive, splitting tensile, flexural strengths, and modulus of elasticity. The findings demonstrated that mechanical characteristics reduced with increased RCA and RAP replacement levels at the same temperature. Moreover, the mechanical characteristic values reduced for the same RCA and RAP replacement ratios when the temperature rises. Katkhuda and Shatarat [1] tested 10 full-scale reinforced concrete (RC) beams without stirrups in an experimental program using three different combinations of coarse aggregates, including natural aggregate (NA), treated RCA, and untreated RCA. The replacement ratios of the RCA in five concrete mixtures differed: 100% NA, 50% treated RCA, 50% untreated RCA, 100% treated RCA, and 100% untreated RCA. The authors reported that employing untreated recycled aggregates decreases the shear capacity of the beams. According to the findings, utilizing 50% RCA improves the beams' shear capacity while using 100% treated RCA decreases the shear capacity of the beams.

Some experimental tests [13, 14] were conducted to examine the bending behavior of recycled concrete beams. Among these studies, limited work is performed on large replacements of the coarse aggregates [15]. Regarding crack morphology and pattern, Pradhan et al. [16] observed no discernible difference between the RC beams made of NA and RCA. However, the authors noted that the specimens with RCA had more cracks than their corresponding NA samples. According to Arezoumandi et al. [17], likely identical crack growth but not crack spacing was observed in the RCA and NA beams tested in flexure. Anike et al. [18] conducted experimental research on RC beams' flexural strength, including recycled fine aggregate (RFA) and RCA with steel fibers (SF). The concrete's hardened density, compressive, and splitting tensile strengths were also investigated. The findings demonstrated that the load-bearing capacity of the specimens with 100% recycled aggregate (RA) and 1% SF prepared by the usual approach increased by up to 13% and 8% compared with a similar mixture without SF and the control mixture, respectively. The nontraditional beam with 60% RA demonstrated the same load resistance (63 kN) as the beam constructed with 100% NA (i.e., control beam). Choi et al. [13] and Zhu et al. [19] examined the structural strength of flexural beams under sustained loads. They also considered the loads that continued for 380 and 3000 days. The creep and shrinkage in concrete substantially influence long-term member behavior. According to Zhu et al. [19], additional systematic testing is necessary to create design techniques.

The finite element (FE) approach can model RC members considering the actual properties of concrete and steel. However, this approach requires considerable computing time and careful assessment of the results. Accordingly, this approach is used to expand the range of experimental tests. In almost all cases, the FE is used in three-dimensional (3D) analysis because it is more accurate when modeling nonlinear behavior [20, 21]. FE simulation is a viable alternative to experimental and theoretical analysis for forecasting the behavior of composite beams [22], particularly when numerous parameters and experimental tests cannot address them individually.

The structural design codes of different countries provide engineers with information and guidelines for designing different structural components. The provisions for evaluating beam resistance (shear and flexural strength) and the other code specifications for durability, details, etc. could show some differences across the codes. Numerous comparative examinations of the provisions found in various design codes are covered in the available literature. However, the data available to verify code provisions for shear and flexure capacity are limited, especially the RCA influences on the shear and flexural behavior of the RC beams. In this

study, various building codes from the USA, Saudi Arabia, and Egypt are evaluated regarding shear and flexural strength, especially with RCA.

Given that RCA performance may change with increased concrete compressive strengths, how the inclusion of RCA influences the shear and flexural behavior of RC beams to establish accurate design methodologies must be understood. This project aims to assess the flexure and shear provisions of three different codes in the context of beams made from recycled aggregate concrete. To fill this gap, this work intends to study a green concrete option through modeling by using the FEs to test the recycled concrete beams that fail in shear and flexure. This study also intends to perform a parametric study using the ABAQUS FE program to address the shortcomings in the available experimental research. Specifically, these shortcomings are the use of relatively small amounts of RA, relatively low concrete compressive strength, relatively high shear reinforcement, and relatively low flexural reinforcement. Sixty FE models with different parameters, including various coarse natural aggregate replacement levels (i.e., 0%, 25%, 50%, 75%, and 100%), compressive strengths (i.e., 25, 35, and 40 MPa); and reinforcement rebar diameters (i.e., 14, 16, and 18 mm), are numerically investigated. Finally, additional experimental results reported in the literature (30 for shear and 61 for flexural tests) are utilized to verify the American Concrete Institute code (ACI318-19) [23], the Saudi Building Code (SBC304-18) [24], and the Egyptian Code of Practice (ECP203-2020) [25] provisions for shear and flexure capacity.

2. Previous Experimental Study

Two beams that had previously been experimentally tested were selected to validate the FE models in the study. The first beam was used to validate the shear performance of the FE models, while the second beam was used to validate the flexural performance of the FE models.

2.1. Shear beam

The FE models of this investigation are validated using the experimentally tested beams from Ignjatovic et al.'s [26] research, namely RAC50-3, with details presented in Figure 1. In this beam, the RCA replaces 50% by mass of the natural coarse aggregate. The shear reinforcement ratio is 0.14%. The concrete cylinder's compressive strength is 37.04 MPa, the Young's modulus is 24.5 GPa, and the splitting tensile strength is 3.2 MPa. The dimensions of the beam are 200 x 300 x 3500 mm. The yield strength of the stirrups is 300 MPa, while that of the longitudinal bars is 555 MPa. The beam is supported and spans a length of 3000 mm. Two-point loads are applied at the third points.

2.2. Flexural beam

The FE models of this investigation are validated using experimentally tested beams from Seara-Paz et al.'s [15] research, namely H50-100, with details presented in Figure 2. In this beam, 100% of the coarse aggregate is replaced by RCA. The beam dimensions are 200 x 300 x 3600 mm. The longitudinal reinforcements are two bars of 16 mm diameter. The beam is supported under two-point loading. The clear span is 3400 mm. The concrete cylinder's compressive strength is 42.9 MPa, the splitting tensile strength is 2.3 MPa, and the Young's modulus is 25.9 GPa. The dimensions and reinforcements of the beam are shown in Figure 2. The yield strength of the stirrups is 240 MPa, while that of the longitudinal bars is 420 MPa.

3. FE Simulation Technique

In the numerical analysis, ABAQUS FE program (version 6.19) [20] was utilized because it can simulate problems with difficult tasks and the nonlinear behavior of various materials, both of which are required for this study.

3.1. Material constitutive model

3.1.1. Modeling of concrete

The concrete damaged plasticity model (CDPM) is frequently used in FE modeling, as done by Alshaikh et al. [27] when modeling the collapse of a frame made of rubberized concrete, by Altheeb et al. [28] when studying the progressive collapse of reinforced concrete

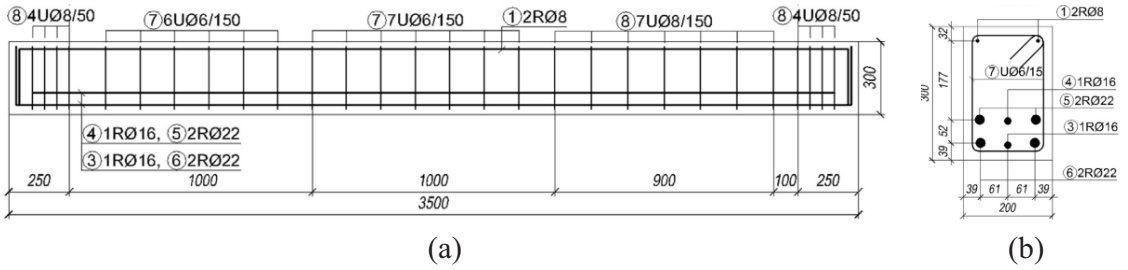

Fig. 1. RAC50-3 specimen details: (a) longitudinal-section and (b) cross-section [26]

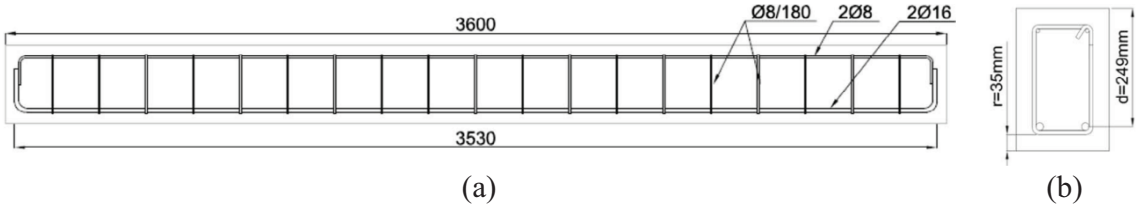

Fig. 2. H50-100 specimen details: (a) longitudinal-section and (b) cross-section [15]

structures, and by Alshaikh et al. [29] when evaluating the progressive collapse of beam-slab substructures made of rubberized concrete, was used in simulating the behavior of concrete. The CDPM accurately simulates how concrete responds to pressure by crashing and cracking, which represented the compressive and tensile strengths, respectively. The CDPM was developed by Lubliner et al. [30] and Lee and Fenves [31]. The CDPM's parameters were chosen in accordance with ABAQUS (Table 1) [20]. The stress-strain curve for the concrete's compression behavior can be split into two portions, as shown in Figure 3. Up to 40% of the maximum compressive strength (f'_c), the first portion, of the curve was ascending, exhibiting a linear elastic response. The second portion of the curve is rising until the stress value reaches the f'_c, which is the nonlinear plastic response. Then, the curve starts to descend due to the decline in concrete strength (Fig. 3). Numerous scholars have proposed a model equation to form the stress-strain curve of typical concrete [32, 33]. The equation recommended by the Eurocode (EN:1992-1-1:2004 [34]) was used in this study.

In all the parametric study that follows, the cylinder compressive strength of the concrete with RAC (f'_{RAC}) is taken concerning the cylinder's compressive strength with NA concrete (f'_c) according to the following two relations reported in reference [35]. The first relation is for 20% to 50% coarse aggregate replacement. The second relation is for 100% coarse aggregate replacement. The other values are obtained as ratios from those of the Equations (1) and (2):

$$f'_{RAC} = 1.19\, {f'_c}^{0.93}, \quad \text{for replacement ratios from 20\% to 50\%} \tag{1}$$

$$f'_{RAC} = 1.16\, {f'_c}^{0.92}, \quad \text{for replacement ratios of 100\%} \tag{2}$$

The expression for the strain at peak strength (ε_{c1}) is given in Figure 3 for concrete with normal aggregates. Also, the maximum value for strain (ε_{cu}) is given as 0.0035. For the case of concrete with recycled aggregates Belen et al. [36] suggest the following relations (Equations (3) and (4)) for the corresponding values of strain at peak strength with recycled aggregates (ε_{c1}^{RAC}) and maximum value for strain with recycled aggregate (ε_{cu}^{RAC}), where %RA is the percentage of coarse recycled aggregate replacement.

$$\varepsilon_{c1}^{RAC} = (0.0021 * \%RA + 1)\varepsilon_{c1} \tag{3}$$

$$\varepsilon_{cu}^{RAC} = (0.0022 * \%RA + 1)\varepsilon_{cu} \tag{4}$$

Table 1. CDPM parameters utilized in this study

Parameters	Dilation angle (ψ)	Stress ratio (f_{b0}/f_{c0})	Compressive meridian (K_c)	Eccentricity (ε)	Viscosity (μ)
Value	27 (calibrated value)	1.16 (default value [20])	0.667 (default value [20])	0.1 (default value [20])	0.001 (default value [20])

The value of the elastic modulus for recycled aggregate concrete (E_c^{RAC}) is given in the experimental work. However, Belen et al. [36] give the following relation (Eq. (5)) in terms of the elastic modulus of the corresponding natural aggregate concrete (E_c).

$$E_{c1}^{RAC} = (1 - 0.002 * \%RA)E_c \tag{5}$$

The value of the modulus of elasticity for the concrete of normal aggregate is taken according to ACI318M-19 [23] as

$$E_c = 4700\sqrt{f_c'} \tag{6}$$

According to Figure 4, which shows the behavior of concrete under tension, the softening curve started with the ultimate concrete tensile strength (f_r), which was estimated according to ACI 318M-19 [23] using Equation (7). In addition, f_r is the stress that determines the initiation of microcracking. Moreover, the fracture energy (G_f) and critical crack opening (W_c) were estimated using Equations (8) and (9), respectively, according to [37, 38].

$$f_r = 0.62\sqrt{f_c'}, \tag{7}$$

$$G_f = 2.5\alpha_0\left(\frac{f_c'}{0.051}\right)^{0.46}\left(1 + \frac{d_a}{11.27}\right)^{0.22}\left(\frac{w}{c}\right)^{-0.3}, \tag{8}$$

$$w_c = 2\frac{G_f}{f_r}, \tag{9}$$

where α_0 is related to the aggregate's types, which is a set of 1.44 crushed or angular aggregates; d_a is related to the aggregate's size, which is a set of 14 mm; and w/c refers to the water-to-cement ratios taken according to each experimental data.

According to reference [35], the tensile strengths for concrete with aggregate replacements of 20%, 50%, and 100% are reduced by 2%, 2%, and 10%, respectively, compared with the concrete with NA. The ratios for the other values of aggregate replacements can be obtained as a percentage from the previously mentioned values.

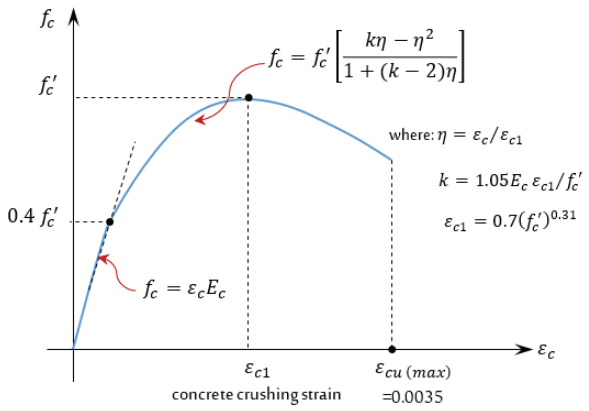

Fig. 3. Stress–strain curve equations for the concrete's compression behavior [34]

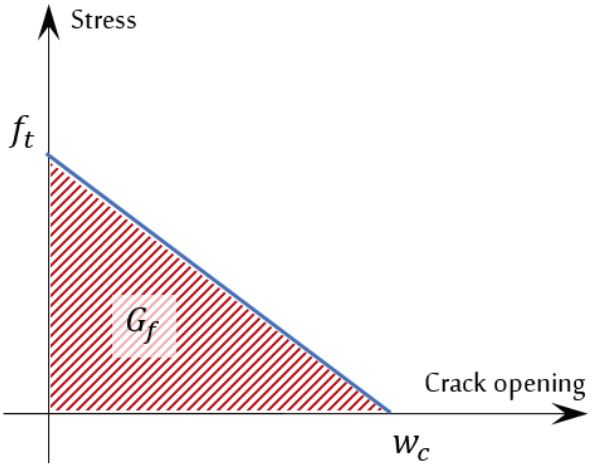

Fig. 4. Concrete's tension behavior

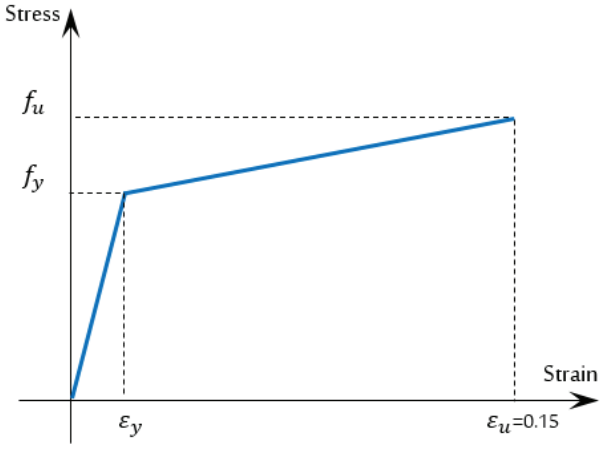

Fig. 5. Idealized curve of the reinforcement bars

3.1.2. Modeling of the reinforcement bars

Titoum et al. [39] presented an idealized bilinear stress-strain curve to simulate the behavior of the reinforcement bars, as shown in Figure 5. The stress-strain curve was generated by utilizing the experimental yield stress value (f_y) and ultimate stress (f_u), which can be set as $1.25f_y$, with yield strain (ε_y) that can be estimated as a modulus of elasticity (E_s) divided by f_y and ultimate strain (ε_u), which is set as 0.15 [40]. The value of each f_y was taken from the experimental data. The idealized curve was employed in this study because it is much more stable to use in a numerical simulation. The E_s and Poisson's ratio (v) for the reinforcement bar were set at 200,000 MPa and 0.3, respectively, which were widely used in FE analysis.

3.2. Finite elements

The concrete beams in each specimen are modeled using continuum elements, which are solid cube-shaped elements. The element, called C3D8R, is 3D, has eight nodes, has reduced integration points to reduce the analysis time, and significantly lowers the computational cost. Reinforcement steel bars are modeled using a truss element (i.e., T3D2), defined as 3D with two node elements. The diameters of all longitudinal and transverse reinforcement bars and the cross-sections of the concrete beams are modeled according to the data presented by Ignjatovic et al. [26] and Seara-Paz et al. [15] for shear and flexural tests, respectively.

3.3. Constraints and interactions

The steel loading and support plates were set as rigid bodies, restricted to the respective reference points, as shown in Figure 6(a). The steel loading and support plates were simulated using only elastic behavior (i.e., $E_s = 200,000$ MPa and $v = 0.3$). The interaction between the steel loading/support plates and the concrete beam surfaces was set to "tie" contact to avoid the convergence problem in the static analysis, as shown in Figure 6(b). The "embedded modeling" technique was used in this study to accurately represent the bonding interaction of the reinforcement steel bars inside the concrete beam, as shown in Figure 6(c). The bonded interaction was applied by restricting the translational degrees of freedom of the embedded elements (i.e., reinforcement bars) to those in the host elements (i.e., surrounding concrete) [20].

3.4. Boundary conditions and loading application

The support characteristics of the experimental tests were applied to the FE models through the boundary condition technique. The boundary conditions and the loading application for each specimen are shown in Figure 7. The transitions and rotations were restricted to represent a hinge for the left support (i.e., U_x=U_y=U_z=UR_x=$UR_y = 0$) and a roller for the right support (i.e., U_y=U_z=UR_x =$UR_y = 0$). The experimental loading was applied to the two steel loading plates by increasing the displacement at their reference points (which act vertically downward) until the specimen failed.

3.5. FE mesh convergence

After modeling, the H50-100 beam was used for the mesh convergence analysis, which was carried out on three various mesh densities (Mesh 1 = size 100 mm, Mesh 2 = size 60 mm, Mesh 3 = size 40 mm, and Mesh 4 = size 20 mm). The results are shown in Figure 8. The four mesh densities were simulated using equal geometry,

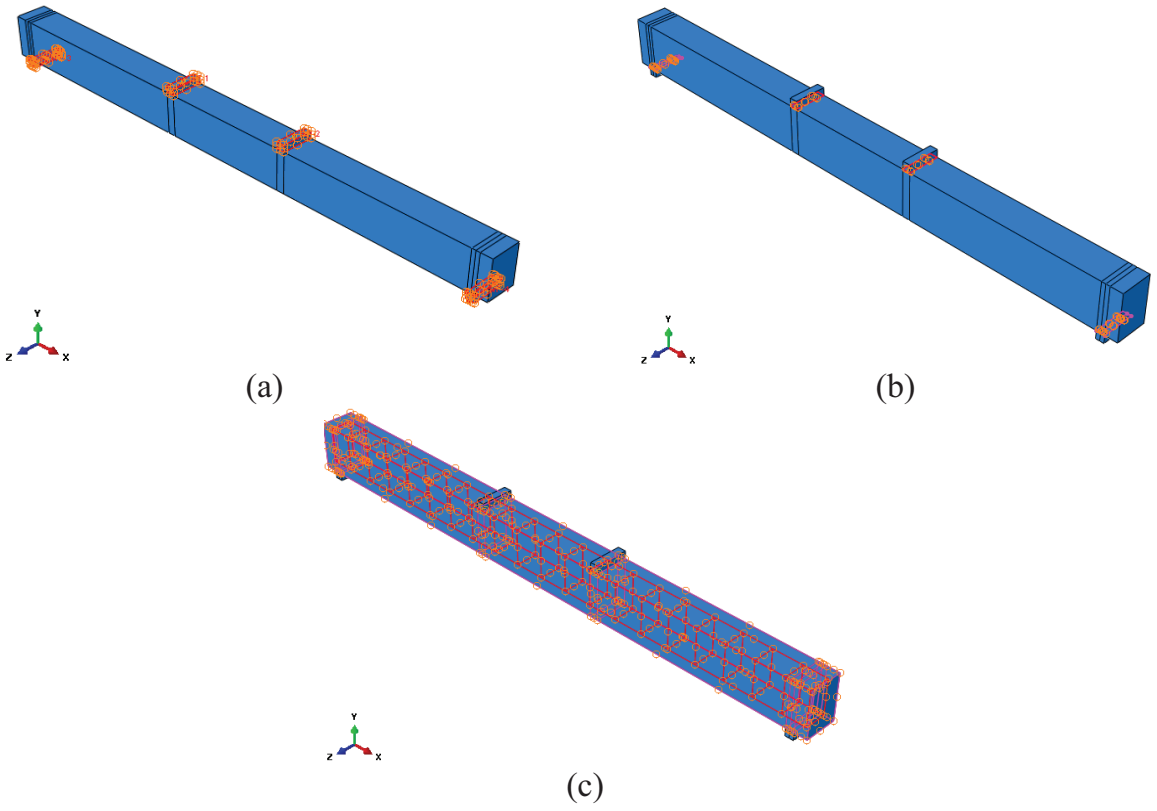

Fig. 6. Constraints and interactions of tested specimens: (a) Rigid bodies, (b) Tie contact, and (c) Embedded constraints

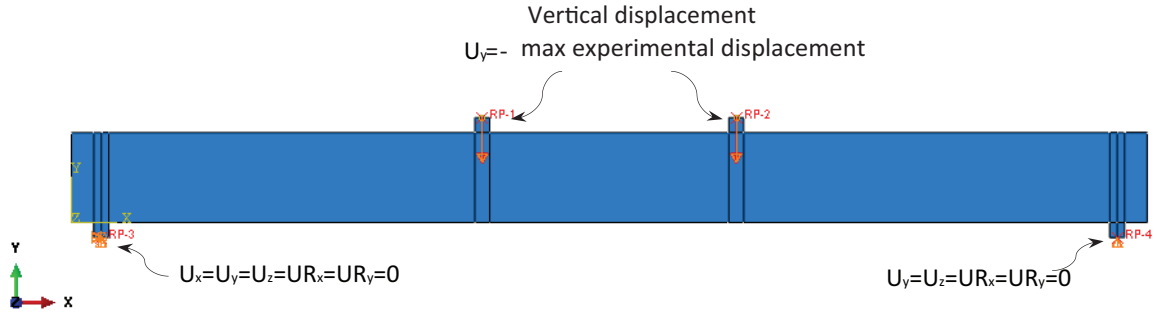

Fig. 7. Boundary conditions and applied loads

material parameters, and FE element types. An assessment of the four mesh densities was carried out to choose a fitting size. Compared with the previous experimental results, Mesh 3 offered a better-fit curve and produced more precise results (Fig. 8). Although Mesh 4 was the smallest size, it did not give better results compared with Mesh 3. Further mesh refinement attempts required more running time and resources. However, these attempts did not improve the results compared with those of Mesh 3. Thus, all the beams (for shear and flexural tests) were adopted at the same size as Mesh 3.

4. Validation of FE Modeling

Figure 9 shows the comparison between the previous experimental and FE load-deflection curves of beam RAC50-3. The FE curve shows

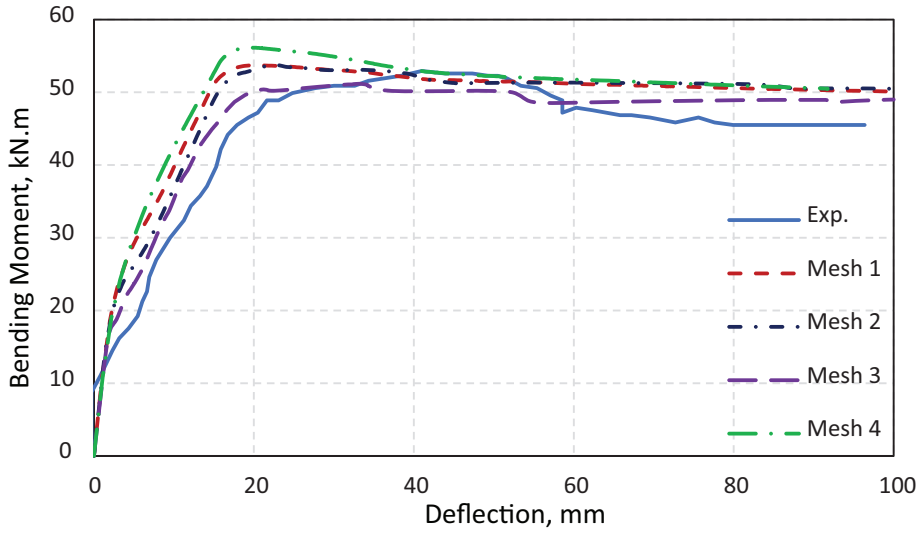

Fig. 8. FE mesh sensitivity results

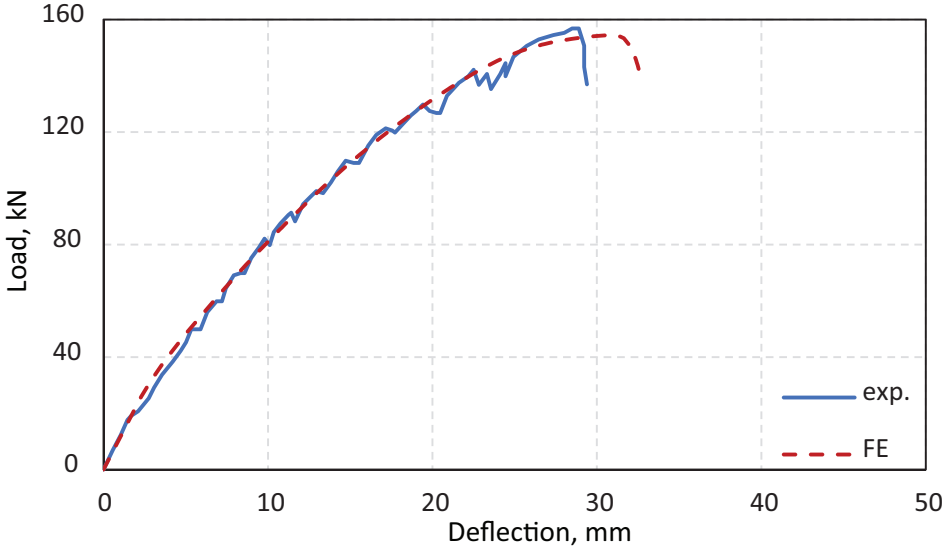

Fig. 9. Experimental and FE load–deflection curves of beam RAC50-3

good agreement. This finding confirms that the FE model using ABAQUS can simulate the shear behavior of this type of beam. Figure 10 presents the comparison of the bending moment–deflection curves of beam H50-100 from the experimental and FE analyses. The close correspondence is evident. The capability of the FE model using ABAQUS to predict the bending behavior is confirmed. Therefore, using various parametric studies, the FE models using ABAQUS software can be applied to investigate the shear and flexural strengths of the RC beams made with RCA.

5. Parametric Study

Fifteen FE runs are performed for beams that failed in shear. The beams have the same cross-section, span, bottom and top reinforcement, supports, and loading as beam RAC50-3 of Ignjatovic et al. [26]. The beams have five recycled

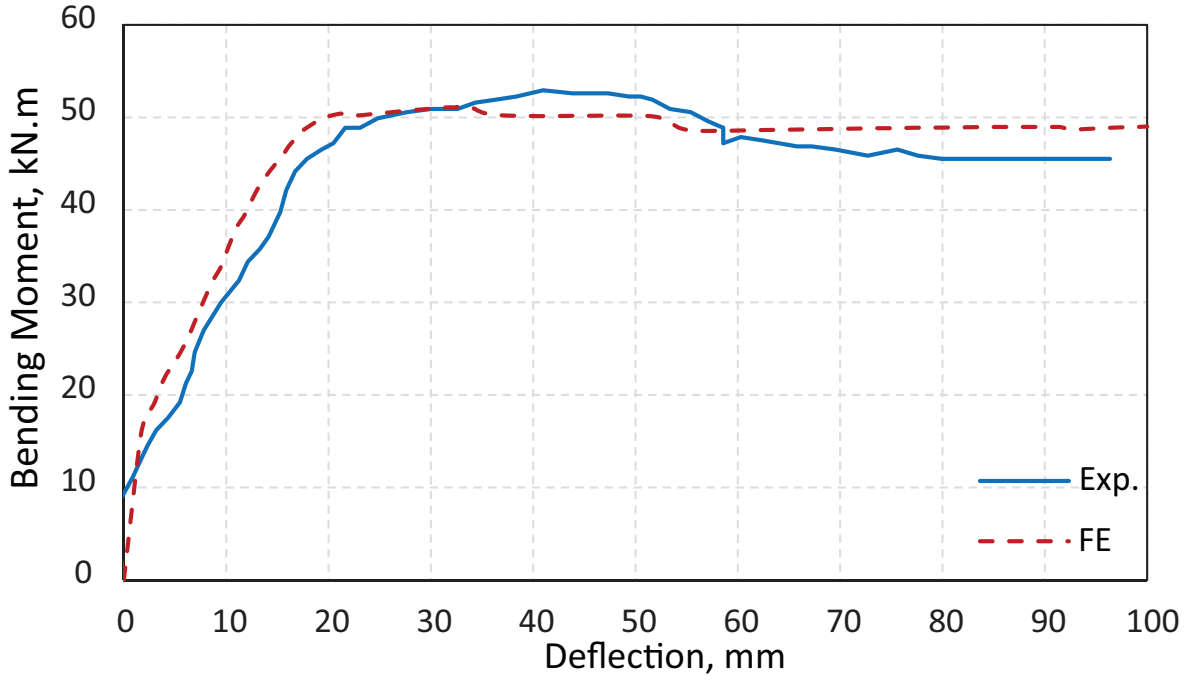

Fig. 10. Experimental and FE bending moment–deflection curves of beam H50-100

aggregate replacement ratios (0%, 25%, 50%, 75%, and 100%). The shear reinforcement consists of stirrups 6 mm in diameter at 150 mm. Three normal aggregate concrete strengths (25, 35, and 40 MPa) are assumed. Moreover, 45 FE runs are performed for beams that failed in flexure. These beams are similar to beam H50-100 of Seara-Paz et al. [15] in terms of the cross-section, span, top reinforcement, stirrups, supports, and loading. The concrete strengths and recycled aggregate ratios are similar to the shear beams. However, the bottom reinforcements are two bars of 18, 16, or 14 mm diameter. The following procedure is used to specify the names of the FE runs conducted in the parametric study. The first letter for shear specimens is S, the second numeral is the ratio of the recycled aggregate replacements. The third numeral is the spacing between stirrups, and the fourth numeral is strength for the case of no recycled aggregates. Regarding the flexural FE runs, the first letter is F, the second numeral is the ratio of the recycled aggregate replacements, the third numeral is the reinforcement diameter, and the fourth numeral is the cylinder concrete compressive strength for the case of no recycled aggregates. The FE analysis matrix that was considered for this study is listed in Table 2.

6. Experimental Results Collected from Literature

Shear and flexural failing beams are collected from the published experimental tests. The compilation consists of 30 experimental beams that failed due to shear, including nine beams with no recycled aggregate for comparison, and 61 experimental beams that failed due to flexure, which include 22 beams with no recycled aggregate for comparison. The 30-shear beams consist of three beams from Ignjatovic [41], four beams from Ajdukiewicz and Kliszczewicz [42], three beams from Fathifazl et al. [43], six beams from Gonzalez-Fonteboa and Martinez-Abella [44], three beams from Ignjatovic et al. [26], two beams from Al Mahmoud et al. [45], and nine beams from Etxeberria [46]. The 61 flexural beams are taken from the previous research work and consist of eight beams from Kang et al. [47], nine beams from Ignjatovic et al. [14], two beams from Choi et al. [13], eight beams from

Table 2. Details of the FE analysis matrix

Scenarios	Specimen ID	RCA ratio	Concrete strengths	Main rebar diameter	No. of specimens
Beams Failing in Flexural	F-0-18-(25/35/40)	0%	25/35/40 MPa	2T18 mm	3
	F-25-18-(25/35/40)	25%			3
	F-50-18-(25/35/40)	50%			3
	F-75-18-(25/35/40)	75%			3
	F-100-18-(25/35/40)	100%			3
	F-0-16-(25/35/40)	0%	25/35/40 MPa	2T16 mm	3
	F-25-16-(25/35/40)	25%			3
	F-50-16-(25/35/40)	50%			3
	F-75-16-(25/35/40)	75%			3
	F-100-16-(25/35/40)	100%			3
	F-0-14-(25/35/40)	0%	25/35/40 MPa	2T14 mm	3
	F-25-14-(25/35/40)	25%			3
	F-50-14-(25/35/40)	50%			3
	F-75-14-(25/35/40)	75%			3
	F-100-14-(25/35/40)	100%			3
Beams Failing in Shear	S-0-150-(25/35/40)	0%	25/35/40 MPa	2T16 + 4T22	3
	S-25-150-(25/35/40)	25%			3
	S-50-150-(25/35/40)	50%			3
	S-75-150-(25/35/40)	75%			3
	S-100-150-(25/35/40)	100%			3
Total Number of Specimens					60

Fathifazl et al. [48], 12 beams from Knaack and Kurama [49], eight beams from Seara-Paz et al.'s [15], four beams from Nandhini et al. [50], and 10 beams from Sato et al. [51]. In the selection of the experimental results, the beams with no stirrups are not considered among the 30 and 61 specimens. These beams cover a wide range of the parameters studied in this research. The cylinder compressive strength of the shear beams ranges from 30 MPa to 50 MPa, and the percentage of used recycled aggregates ranges from 30% to 100%. However, the cylinder compressive strength of the flexural beams ranges from 29 MPa to 57 MPa, and the percentage of recycled aggregates used for these collected beams varies from 20% to 100%.

7. Analysis of Results

7.1. Shear beams

7.1.1. Effect of recycled aggregate ratio

The beams of the parametric study, which are made using FE runs, are grouped based on the strength of the beams with normal aggregates. Every group consisted of five beams with similar parameters, except the recycled aggregate ratio. Figure 11 shows, for one group as an example, the variation of load and deflection for beams with recycled aggregate ratios' replacements equal to 0%, 25%, 50%, 75%, and 100%, and the normal concrete strength of 25 MPa. The maximum load decreased with the increase in the RCA ratio, and the deflection increased. The curves' ascending portion was similar, up to around 40% of the maximum loads. The descending parts after the maximum loads were similar. This phenomenon can be attributed to the shear resistance of the specimens with RCA being adversely affected by its high-water absorption [52] and higher porosity because the adhered mortar stuck to the NA, which could result into a greater permeability interfacial transition zone between the adhered mortar and NA [53]. Replacing 25% of the NA with RCA resulted in a decrease in shear strength of an average of 4.1% for all different concrete strengths (i.e., 25, 35, and 40 MPa) compared with the specimens without RCA.

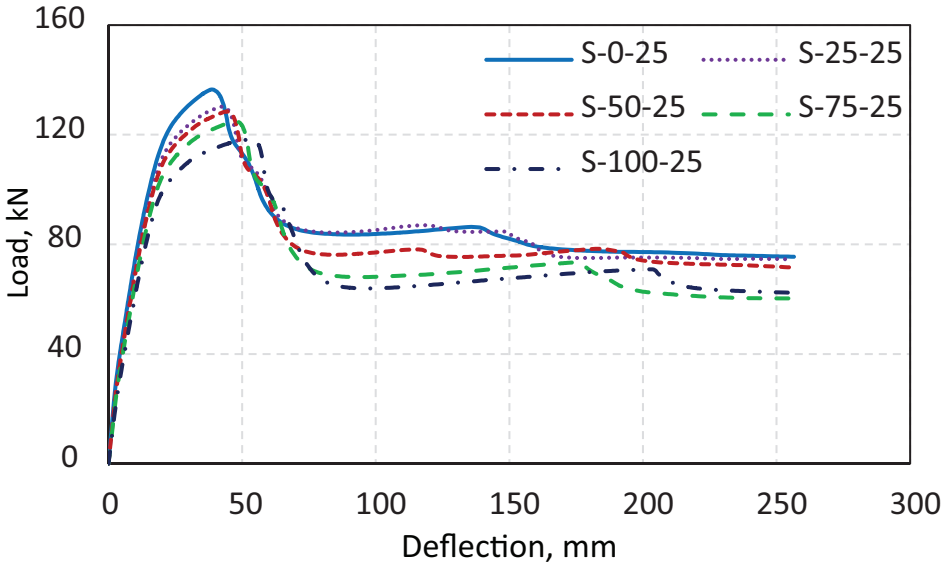

Fig. 11. Load–deflection relationships for beams with different RCA ratios

The same pattern was observed in the increased RCA ratios, which resulted in a decrease in the shear strength with averages of 5.5%, 8.2%, and 10.1% for specimens with replacement levels of 50%, 75%, and 100%, respectively, with all different concrete strengths (i.e., 25, 35, and 40 MPa) compared with the specimens without RCA. The investigation results in this study were consistent with those of previous studies [1, 12]. Moreover, cohesive strength, interfacial friction strength, and aggregate interlocking strength comprised most of the shear strength of RCA specimens, with interfacial friction strength dominating and accounting for 25% to 70% of the strength of the RCA specimens for shear [54].

7.1.2. Effect of concrete strength

In this study, the beams were grouped based on the ratio of recycled aggregate replacements. Every group contained three beams of different compressive strengths for the corresponding beams of no recycled aggregates. One group is presented in Figure 12, which presents the relation between load and deflection for three beams with recycled aggregate replacements of 50% and different concrete strengths. The three curves were similar, up to 40% of the maximum load. Decreased concrete strength resulted in a lesser load capacity and greater deflection. The results indicated that increasing the strength of concrete results in an increase in shear strength. This result is consistent with the codes' prediction of the concrete shear strength of beams [23–25]. Using concrete with 35 MPa strength resulted in a 16.6% increase ratio. Meanwhile, the utilization of concrete with 40 MPa strength increased by 23.1% compared with the specimens with concrete with 25 MPa strength. A slight decrease in shear strength was observed when concrete with 35 MPa strength was used compared with that with 40 MPa strength (Fig. 12). The specimens with 35 MPa strength recorded an average decrease of only 6.3%. Meanwhile, the specimens with 40 MPa strength recorded an average decrease of only 6.6% compared with other specimens without RCA.

7.2. Flexural beams

7.2.1. Effect of recycled aggregate ratio

The beams of the FE runs are grouped based on the bottom reinforcement and compressive strength of the corresponding concrete beam of normal aggregates. Each group contains five beams with five different recycled aggregate replacements (0%,

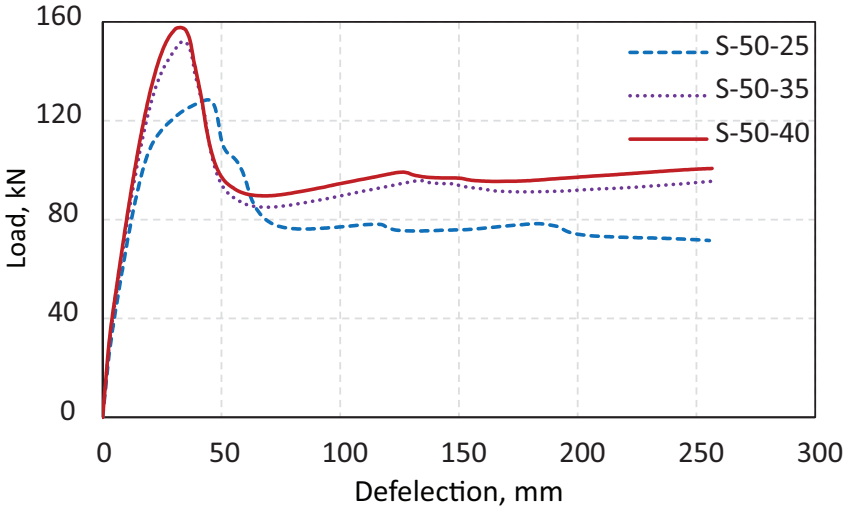

Fig. 12. Load–deflection relationships for beams with different concrete strengths

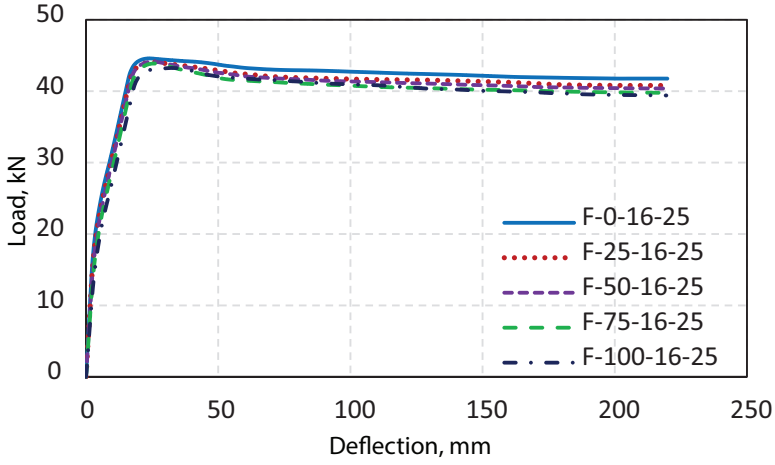

Fig. 13. Load–deflection relationships for beams with different RCA ratios

25%, 50%, 75%, and 100%). The load-deflection relationships for beams with bottom reinforcement of two bars with 16 mm diameter and 25 MPa concrete strength for the corresponding normal aggregate concrete are shown in Figure 13. The effect of the RCA ratio on the flexural capacity is limited because the flexural capacity is mainly affected by the reinforcement rebars. This result can be attributed to the behavior of the under-reinforced beams being governed by the reinforcement ratio rather than the properties of the concrete [55]. Almost all the curves are similar at all stages. Replacing 25%, 50%, 75%, and 100% of the NA with the RCA resulted in a reduction in the flexural capacity of only averages of 1.1%, 1.4%, 1.8%, and 3.3%, respectively, for all different concrete strengths (i.e., 25, 35, and 40 MPa) and the 18 mm rebar diameter compared with the specimens without RCA. In addition, the same pattern was observed in the use of 16 mm rebar diameter, which resulted in a decrease in the flexural capacity with averages of 0.9%, 1.3%, 0.9%, and 3.3% for specimens with replacement levels of 25%, 50%, 75%, and 100%, respectively, with all different concrete strengths (i.e., 25, 35, and 40 MPa) compared with the specimens without RCA. Moreover, replacing

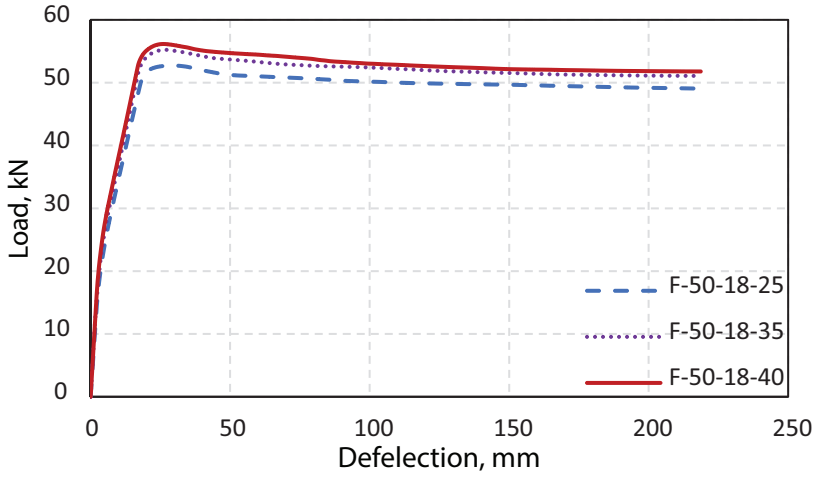

Fig. 14. Load–deflection relationships for beams with different concrete strengths

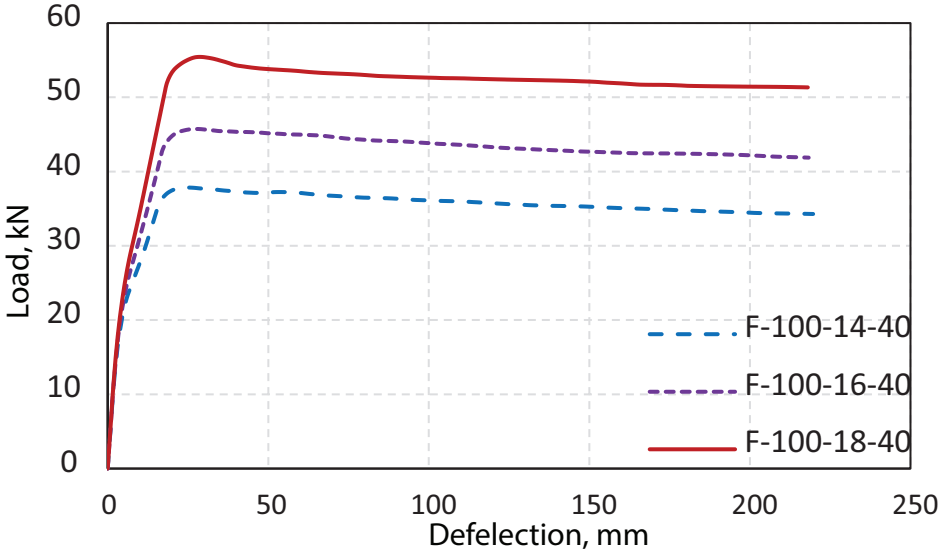

Fig. 15. Load–deflection relationships for beams with different reinforcement rebars

25%, 50%, 75%, and 100% of the NA with the RCA resulted in a reduction in the flexural capacity of only averages of 1.1%, 1.8%, 1.9%, and 3.1%, respectively, for all different concrete strengths (i.e., 25, 35, and 40 MPa) and for 14 mm rebar diameter compared with the specimens without RCA. The investigation results in this study are consistent with those of previous studies, wherein the authors reported that the failure mode and crack pattern in the specimens with RCA are similar to those without RCA, regardless of the RCA content [14, 42]. The results indicated that increasing the strength of the concrete slightly increased the flexural capacity, as shown in Figure 14. Concerning the use of 18 mm rebar diameter, the utilization of concrete with 35 MPa strength exhibited a 4.8% increase ratio. In contrast, using concrete with a 40 MPa strength resulted in a 6.4% increase compared with the specimens with concrete with 25 MPa strength. The same pattern was observed when a 16 mm rebar diameter was utilized, resulting in an increase in the flexural capacities of 4.5%

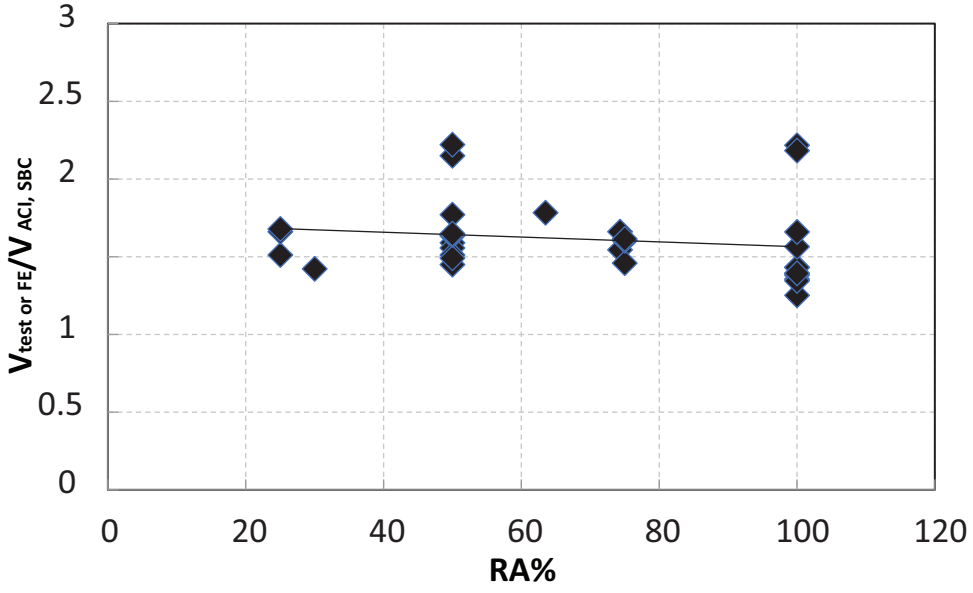

Fig. 16. Relationship between the ratio of shear from test or FE to shear from the ACI318-19 and SBC304-18 codes and percent of RCA

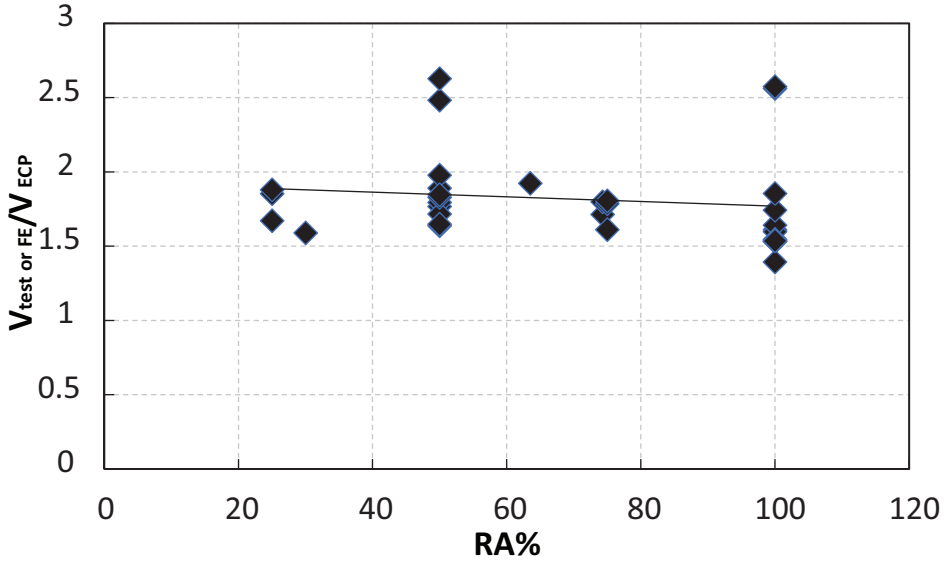

Fig. 17. Relationship between the ratio of shear from the test or FE to shear from the ECP203-2020 codes and the percent of RCA

and 6.4% for specimens with concrete with 35 MPa strength and concrete with 40 MPa strength, respectively, compared with the specimens with concrete with 25 MPa strength. Moreover, using 14 mm rebar diameter with concrete with 35 MPa strength exhibited a 5.3% increase ratio. Meanwhile, using concrete with 40 MPa strength resulted in a 7.5% increase compared with the specimens with 25 MPa strength. Using 18 mm of rebar diameter exhibited an average 46.1% increase

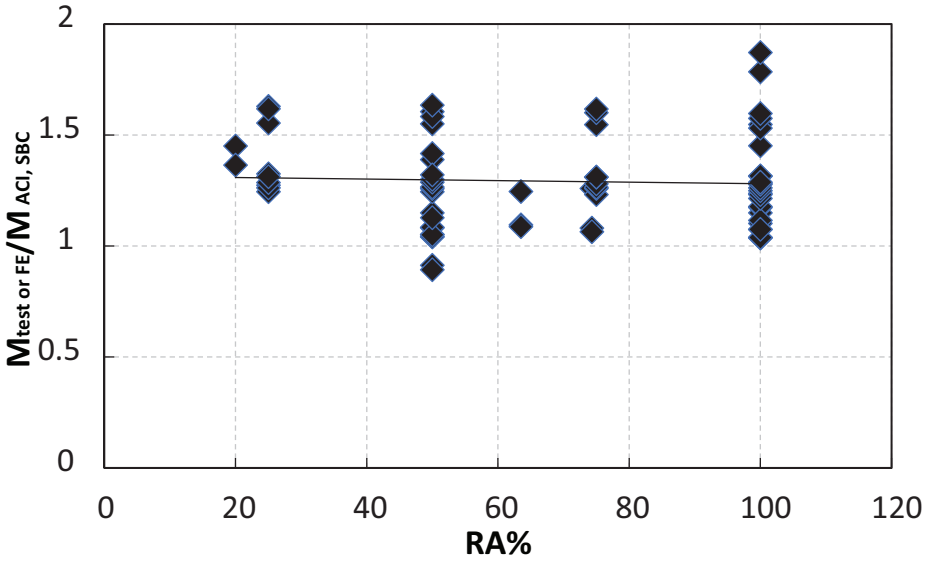

Fig. 18. Relationship between the ratio of moment capacity from the test or FE to moment capacity from the ACI318-19 and SBC304-18 codes and the percent of RCA

ratio. Meanwhile, the use of 16 mm rebar diameter resulted in an average of 21.6% increase for all different concrete strengths (i.e., 25, 35, and 40 MPa) compared with the specimens with 14 mm rebar diameter, as shown in Figure 15.

8. Comparing the Experimental and FE Results with Code Predictions

8.1. Shear results

The failure shear loads for the 15 FE runs using ABAQUS and 25 tests collected from literature are recorded and compared with those calculated from the ACI318-19 [23], SBC304-18 [24], and ECP203-2020 [25] codes. Figures 16 and 17 present the relationships between the ratios of shear from the test or FE and the shear calculated from the ACI318-19, SBC304-18, or ECP203-2020 code and the percent of RCA content. The errors obtained when using the three codes for calculating the shear capacity compared with the values from the FE or the tests are recorded. The average error obtained for the beams with RCA is 58% using the ACI318-19 and SBC304-18 codes and 78% utilizing the ECP203-2020. Meanwhile, the average error of the beams without RCA, which is not shown in the figures, is 58% using the ACI318-19 and SBC304-18 and 79% utilizing ECP203-2020. Given that the errors in calculating the shear capacity when using each code for cases of no RCA and with RCA are almost the same, the equations for calculating the shear capacity in the three codes can still be used for concrete with RCA replacements. The shown trend lines in the two figures indicate that the errors decrease with the RCA replacement, indicating less conservatism for the three codes as the ratio of RCA becomes larger.

8.2. Flexural results

The maximum moment capacities were obtained for the 45 FE runs using ABAQUS, and 49 experiments were collected from the literature. These maximum moment capacities were compared with the flexural capacities obtained from the ACI318-19 [23], SBC304-18 [24], and ECP203-2020 [25] codes. The relationships between the ratios of moment capacity from the test or FE to the moment capacity calculated from ACI318-19, SBC304-18, or ECP203-2020 and the percent of RCA content

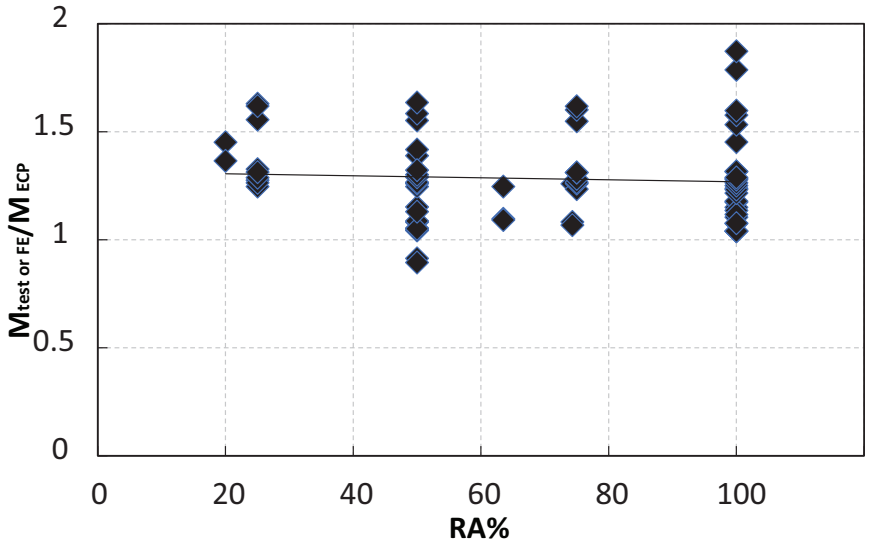

Fig. 19. Relationship between the ratio of moment capacity from the test or FE to moment capacity from the ECP203-2020 codes and the percent of RCA

are shown in Figures 18 and 19, respectively. The errors obtained when using the three codes for calculating the flexural capacity were compared with the values from the tests and FE. The average error obtained for the beams with RCA is 27% using the ACI318-19 and SBC304-18 codes and 26% using the ECP203-2020 code. Meanwhile, the average error of the beams without RCA, which is not shown in the figures, is 21% using the ACI318-19 and SBC304-18 codes and 21% utilizing the ECP203-2020 codes. Given that the errors in the calculated flexural capacities when using the three codes for the two cases of no RCA and with RCA were almost the same, the bending capacity calculations in the three codes can still be used for concrete with RCA replacements. The trend lines shown in the two figures indicated that the errors become smaller, suggesting a reduction in the conservatism of the three codes with the increase in the ratio of RCA.

9. Conclusions

This study investigates the shear and flexural behavior of beams containing RCA using FE simulations with the ABAQUS program. The FE models are validated using previous experimental tests. The finite element parametric study results are added to the existing experimental data reported in the literature and used together to verify the code's provisions for shear and flexure capacity. The conclusions of the study are as follows:

1. The results from the FE models are consistent with the experimental results for RC beams that fail in shear and flexure. The tested beams' results could be accurately and numerically predicted using a nonlinear FE model developed using ABAQUS.
2. The shear strength of the RC beam increases with the increase in the compressive strength from 25 MPa to 40 MPa. This result is consistent with the codes' prediction of the concrete shear strength of beams. The use of concrete with 35 and 40 MPa strength exhibited a 16.6% and 23.1% increase ratio, respectively, compared with the specimens with 25 MPa strength concrete.
3. The maximum load of shear beams decreases with the increase in the RCA level, and the deflection increases. Meanwhile, the decrease in the concrete strength results in lesser capacity and

greater deflection. The reduction in shear strength is an average of 4.1%, 5.5%, 8.2%, and 10.1% for specimens with replacement levels of 25%, 50%, 75%, and 100%, respectively, compared with the specimens without RCA.

4. The effect of the RCA level on the flexural capacity of the flexure beams is limited because the flexural capacity is mainly affected by the reinforcement. The specimens with RCA showed a slight reduction of up to 3.3% when using 16 and 18 mm of rebar diameters, while it was 3.1% when using 14 mm of rebar diameters compared with the specimens without RCA.
5. The work performed in this research proves that the shear strength capacity decreases with an increase in the RCA ratio, while the effect of using RCA on the flexural capacity is limited.
6. The available equations in the ACI318-19, SBC304-18, and ECP203-2020 codes can still be used for calculating the shear and flexural capacities of beams containing RCA—however, the increase in the RCA results in less conservative equations.

The authors suggest that additional investigation is necessary to develop novel approaches for improving the design code provisions for shear and flexure capacity. Additionally, a wider range of concrete strengths should be investigated, together with examining sources of recycled aggregate, to assess their effect on the different design code provisions.

Acknowledgment

The authors extend their appreciation to the Deputyship for Research & Innovation, Ministry of Education in Saudi Arabia for funding this research work through the project number ISP23–131.

References

[1] Katkhuda H, Shatarat N. Shear behavior of reinforced concrete beams using treated recycled concrete aggregate. *Constr Build Mater*. 2016;**125**: 63–71.

[2] Makul N et al. Use of recycled concrete aggregates in production of green cement-based concrete composites: A review. *Crystals*. 2021;**11**(3): 232.

[3] Matias D et al. Mechanical properties of concrete produced with recycled coarse aggregates–Influence of the use of superplasticizers. *Constr Build Mater.* 2013;**44**: 101–109.

[4] Aldmour R, Shatarat N. Biaxial shear behavior of recycled concrete aggregate reinforced concrete beams. *Case Stud Constr Mater.* 2023;**18**: e02127.

[5] Makul N et al. Capacity to develop recycled aggregate concrete in South East Asia. *Buildings*, 2021;**11**(6): 234.

[6] Amin M et al. Influence of recycled aggregates and carbon nanofibres on properties of ultra-high-performance concrete under elevated temperatures. *Case Stud Constr Mater.* 2022;**16**: e01063.

[7] Makul N et al. Design strategy for recycled aggregate concrete: A review of status and future perspectives. *Crystals*. 2021;**11**(6): 695.

[8] Mehta PK, Monteiro P. *Concrete Microstructure, Properties, and Materials.* McGraw-Hill Education, New York, 2014. **4th edn.**

[9] Xiao, J et al. A recycled aggregate concrete high-rise building: Structural performance and embodied carbon footprint. *J Clean Prod.* 2018;**199**: 868–881.

[10] Hakeem IY et al. Properties of sustainable high-strength concrete containing large quantities of industrial wastes, nanosilica and recycled aggregates. *J. Mater Res Technol.* 2023;**24**: 7444–7461.

[11] Al-Tayeb MM et al. Experimental and numerical investigations of the influence of partial replacement of coarse aggregates by plastic waste on the impact load. *Int J Sustain Eng.* 2021;**14**(4): 735–742.

[12] Abedalqader A et al. Influence of temperature on mechanical properties of recycled asphalt pavement aggregate and recycled coarse aggregate concrete. *Constr Build Mater.* 2021;**269**: 121285.

[13] Choi WC, Yun HD, Kim SW. Flexural performance of reinforced recycled aggregate concrete beams. *Mag Concr Res.* 2012;**64**(9): 837–848.

[14] Ignjatović IS et al. Flexural behavior of reinforced recycled aggregate concrete beams under short-term loading. *Mater Struct.* 2013;**46**: 1045–1059.

[15] Seara-Paz S et al. Flexural performance of reinforced concrete beams made with recycled concrete coarse aggregate. *Eng Struct.* 2018;**156**: 32–45.

[16] Pradhan S, Kumar S, Barai SV. Performance of reinforced recycled aggregate concrete beams in flexure: experimental and critical comparative analysis. *Mater Struct.* 2018;**51**: 1–17.

[17] Arezoumandi M et al. An experimental study on flexural strength of reinforced concrete beams with 100% recycled concrete aggregate. *Eng Struct.* 2015;**88**: 154–162.

[18] Anike EE et al. *Flexural performance of reinforced concrete beams with recycled aggregates and steel fibres*. In: Structures. 2022. Elsevier.

[19] Zhu C et al. Study on long-term performance and flexural stiffness of recycled aggregate concrete beams. *Constr Build Mater.* 2020;**262**: 120503.

[20] ABAQUS, *User Assistance.* Dassault Systèmes Simulia Corporation, Providence, Rhode Island, USA., 2019.

[21] Magbool HM, El-Abbasy AA. Finite element verification of the unreliability of using structural plain concrete footing under reinforced concrete footing. *Case Stud Constr Mater.* 2021;**15**: e00734.

[22] Chan R, Moy CK, Galobardes I. Numerical and analytical optimisation of functionally graded concrete incorporating steel fibres and recycled aggregate. *Constr Build Mater.* 2022;**356**: 129249.

[23] ACI. *Building Code Requirements for Structural Concrete (ACI 318–19)*. In: American Concrete Institute. 2019.

[24] SBC304-18. *Concrete Structures Requirements—SBC 304*. In: Saudi Building Code National Committee: Riyadh, Saudi Arabia. 2018.

[25] ECP203-2020. *Egyptian Code for Design and Construction of Reinforced Concrete Structures*. in *Committee for Egyptian Concrete Code*. 2020. Housing and Building National Research Center, Giza, Egypt.

[26] Ignjatović IS, Marinković SB, Tošić N. Shear behaviour of recycled aggregate concrete beams with and without shear reinforcement. *Eng Struct.* 2017;**141**: 386–401.

[27] Alshaikh I.M et al. *Finite element analysis and experimental validation of progressive collapse of reinforced rubberized concrete frame*. In: Structures. 2021. Elsevier.

[28] Altheeb A et al. Effects of Non-Structural Walls on Mitigating the Risk of Progressive Collapse of RC Structures. *Lat Am J Solids Struct.* 2022;**19**.

[29] Alshaikh IM et al. Progressive Collapse Resistance of RC Beam–Slab Substructures Made with Rubberized Concrete. *Build.* 2022;**12**(10): 1724.

[30] Lubliner Jet al. A plastic-damage model for concrete. *Int J Solids Struct.* 1989;**25**(3): 299–326.

[31] Lee J, Fenves GL. Plastic-damage model for cyclic loading of concrete structures. *J Eng Mech.* 1998;**124**(8): 892–900.

[32] Hognestad E. *Study of combined bending and axial load in reinforced concrete members*. 1951. University of Illinois at Urbana Champaign, College of Engineering.

[33] Yi ST, Kim JK, Oh TK. Effect of strength and age on the stress–strain curves of concrete specimens. *Cem Concr Res.* 2003;**33**(8): 1235–1244.

[34] EN:1992-1-1:2004. *Eurocode 2: design of concrete structures-part 1–1: general rules and rules for buildings.* 2005.

[35] El-Latif A. *Structural Behavior of Reinforced Concrete Beams with Recycled Concrete Aggregates*. In: Civil Engineering. Cairo University: Egypt. 2009;154.

[36] Belén GF et al. Stress–strain relationship in axial compression for concrete using recycled saturated coarse aggregate. *Constr Build Mater.* 2011;**25**(5): 2335–2342.

[37] Bažant ZP, Becq-Giraudon E. Statistical prediction of fracture parameters of concrete and implications for choice of testing standard. *Cem Concr Res.* 2002;**32**(4): 529–556.

[38] Coronado CA, Lopez MM. Sensitivity analysis of reinforced concrete beams strengthened with FRP laminates. *Cem Concr Compos.* 2006;**28**(1): 102–114.

[39] Titoum M et al. Analysis of semi-continuous composite beams with partial shear connection using 2-D finite element approach. *Asian J Appl Sci.* 2008;**1**(3): 185–205.

[40] EN:1992-1-2. *Eurocode 2: Design of concrete structures—Part 1–2: General rules—Structural fire design.* European Committee for Standardization. 2004.

[41] Ignjatović I. *Ultimate strength of reinforced recycled concrete beams.* University of Belgrade. 2013;**19**: 20.

[42] Ajdukiewicz AB, Kliszczewicz AT. Comparative tests of beams and columns made of recycled aggregate concrete and natural aggregate concrete. *J Adv Concr Technol.* 2007;**5**(2): 259–273.

[43] Fathifazl G et al. Shear strength of reinforced recycled concrete beams without stirrups. *Mag Concr Res.* 2009;**61**(7): 477–490.

[44] Gonzalez-Fonteboa B, Martínez-Abella F. Shear strength of recycled concrete beams. *Constr Build Mater.* 2007;**21**(4): 887–893.

[45] Al Mahmoud F et al. *Shear behavior of reinforced concrete beams made from recycled coarse and fine aggregates*. In: *Structures*. 2020. Elsevier.

[46] Etxeberria Larrañaga M. *Experimental study on microstructure and structural behaviour of recycled aggregate concrete*. Universitat Politècnica de Catalunya. 2004.

[47] Kang THK et al. Flexural Testing of Reinforced Concrete Beams with Recycled Concrete Aggregates. *ACI Struct J.* 2014;**111**(3).

[48] Fathifazl G et al. Flexural performance of steel-reinforced recycled concrete beams. *ACI Struct J.* 2009;**106**(6).

[49] Knaack AM, Kurama YC. Behavior of reinforced concrete beams with recycled concrete coarse aggregates. *J Struct Eng.* 2015;**141**(3): B4014009.

[50] Nandhini KU et al. Flexural strength properties of recycled aggregate concrete. 2016;**5**(5): 6–11.

[51] Sato R et al. Flexural behavior of reinforced recycled concrete beams. *J Adv Concr Technol.* 2007;**5**(1): 43–61.

[52] Schubert S et al. Recycled aggregate concrete: experimental shear resistance of slabs without shear reinforcement. *Eng Struct.* 2012;**41**: 490–497.

[53] Silva RJ, De Brito, Dhir R. Properties and composition of recycled aggregates from construction and demolition waste suitable for concrete production. *Constr Build Mater.* 2014;**65**: 201–217.

[54] Lei B et al. Mechanical properties of multi-recycled aggregate concrete under combined compression-shear loading. *Eng Fail Anal.* 2023;**143**: 106910.

[55] Visintin P et al. Flexural performance and life-cycle assessment of multi-generation recycled aggregate concrete beams. *J Clean Prod.* 2022;**360**: 132214.

Received 2024-03-20
Accepted 2024-07-14